Journal Pre-proof

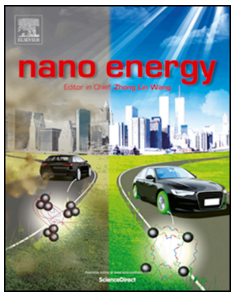

Grid of hybrid nanogenerators for improving ocean wave impact energy harvesting self-powered applications

Ulises Tronco Jurado, Suan Hui Pu, Neil M. White

PII: S2211-2855(20)30258-5

DOI: https://doi.org/10.1016/j.nanoen.2020.104701

Reference: NANOEN 104701

To appear in: *Nano Energy*

Received Date: 28 January 2020

Revised Date: 9 March 2020

Accepted Date: 9 March 2020

Please cite this article as: U.T. Jurado, S.H. Pu, N.M. White, Grid of hybrid nanogenerators for improving ocean wave impact energy harvesting self-powered applications, *Nano Energy*, https://doi.org/10.1016/j.nanoen.2020.104701.

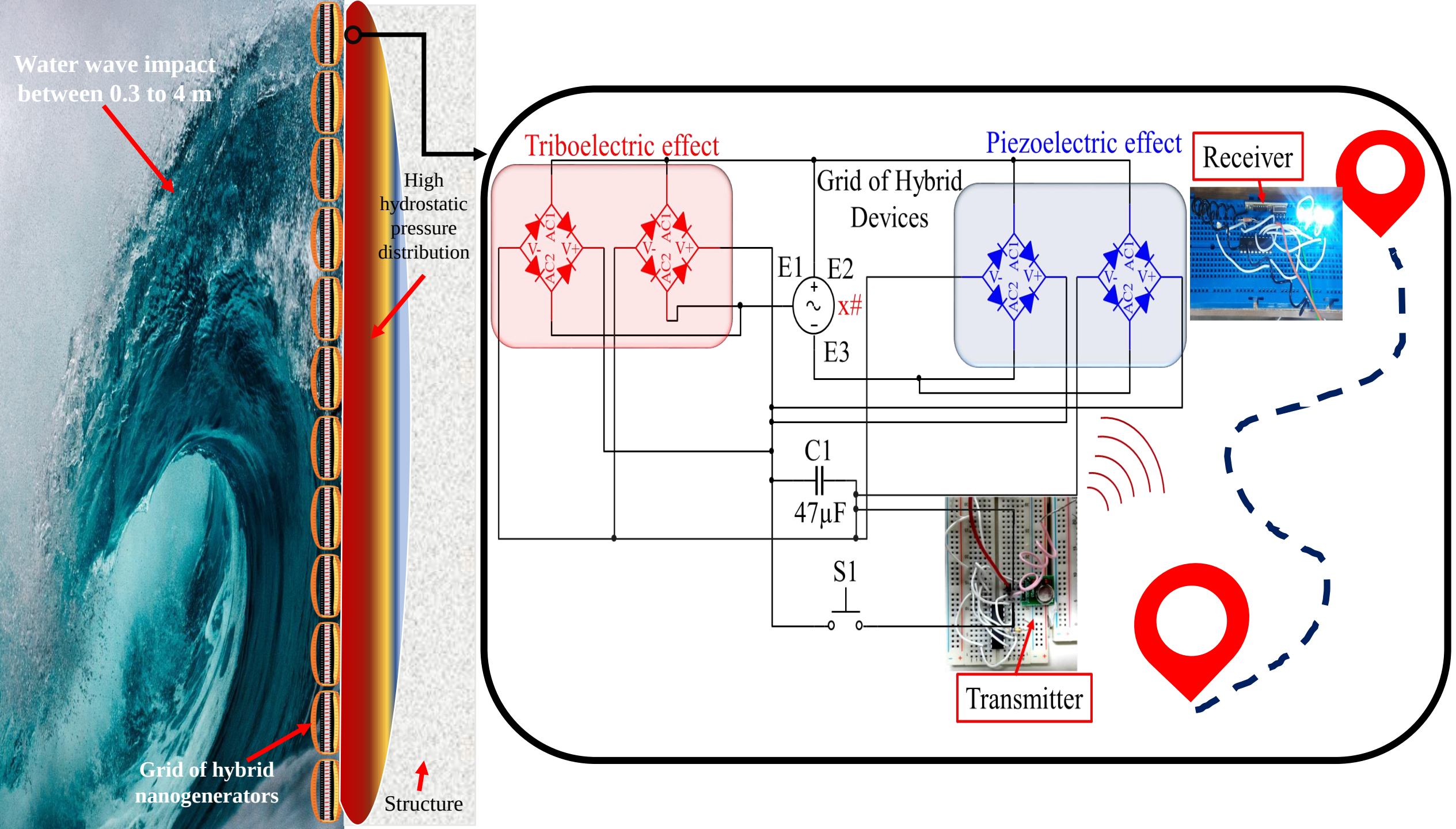
Water wave impact between 0.3 to 4 m
High hydrostatic pressure distribution
Grid of hybrid nanogenerators
Structure
Triboelectric effect
Piezoelectric effect
Grid of Hybrid Devices
E1
E2
E3
x#
C1
47µF
S1
Receiver
Transmitter

Grid of hybrid nanogenerators for improving ocean wave impact energy harvesting self-powered applications

Ulises Tronco Jurado[a, b, *], Suan Hui Pu[a, c], Neil M. White[b]

[a]*Mechatronics Research Group, University of Southampton, Southampton, SO17 1BJ, UK.*
[b]*Smart Electronic Materials and Systems Research Group, University of Southampton, Southampton, SO17 1BJ UK.*
[c]*University of Southampton Malaysia, Iskandar Puteri 79200, Johor, Malaysia.*
[*]*Corresponding author.*
E-mail addresses: utj1n15@soton.ac.uk (Ulises Tronco Jurado), SuanHui.Pu@soton.ac.uk (Suan Hui Pu), nmw@ecs.soton.ac.uk (Neil M. White).

Abstract
This paper describes an alternative approach for improving the output power performance for coastal wave impact energy harvesting systems, located at water-structure interfaces. This is achieved by simultaneously coupling the triboelectric and piezoelectric effects, exhibited in some materials. The use of finite element modelling, and experimental electrical characterization, enables the integration of hybrid devices into a breaking water wave generator tank. This provides a mechanism for simulating actual ocean wave conditions at low frequencies (0.7 Hz – 3 Hz). Enhancements in the output performance by a factor of 2.24 and 3.21, relative to those obtained from using single triboelectric and piezoelectric nanogenerators, were achieved. This is demonstrated by evaluating the output current, voltage, transferred charge, and charging performance from a grid of up to four hybrid devices connected to capacitors of different capacitance values. Such hybrid devices were capable of powering a one-way wireless transmitter with a generated output power between 340.85 µW to 2.57 mW and sent a signal to a receiver at different distances from 2 m to 8 m. The research shows that such an integrated device can provide a promising mechanism for developing high-performance energy harvesting mechanisms for ocean wave impact to drive self-powered systems having an average power consumption of 1 to 100 mW. Further, it is estimated that through the construction of large water-hybrid nanogenerator-structure interfaces, output powers of approximately 21.61 W can be generated for powering networks of self-powered sensing systems in smart large-scale applications.

Keywords: Coastal wave impact, dielectric-conductor, triboelectric-piezoelectric effects, hybrid nanogenerators, marine sensing platforms, water-structure interfaces.

1. Introduction

The energy harvested from the shallow ocean waves has been attracting a great potential as a source of electricity for many years [1]. Specially, different triboelectric nanogenerators (TENG) based on contact electrification of solid-solid and liquid-solid interfaces [2-8], and hybrid devices combined with TENG-electromagnetic generators (EMG) [9, 10] have been developed focusing in harvesting the irregular motions at low frequencies between 0.5 Hz to 5 Hz, generated by the shallow ocean wave energy. Therefore, this work focuses on harvesting the breaking wave impact energy at coastal structures that varies between slowly-acting pulsating loads, and more intense impulsive loads [11], which can be effectively exploited as a source of electrical energy. Two different approaches for harvesting coastal wave impact forces have been demonstrated using a dielectric-metal contact separation mode triboelectric nanogenerators (DMCS-TENG) with solid materials in contact at wide frequency range (30 Hz to 252 Hz) [12, 13], and also water-dielectric contact [14] using water as a triboelectric material at low frequency range (1.2 Hz). However, as further investigation is required to explore suitable designs of TENG with engineering challenges to improve the energy conversion efficiency harvesting the breaking ocean wave impact. This research proposes an alternative approach, stable, ease, simple to fabricate, and lightweight hybrid nanogenerator to promote the output current to improve the low output power of DMCS-TENG harvesting the impact of the water waves as previously studied [12-15]. Focused at low frequency impact among 0.7 Hz to 3 Hz, by integrating a polyvinylidene fluoride (PVDF) piezoelectric layer [16, 17] with suitable chosen triboelectric material pairs [13, 18-20].

Firstly, the simultaneous operation of triboelectric-piezoelectric effects [21-23] under water wave impact was studied. The hybrid nanogenerator energy harvesters utilize dielectric-to-conductor triboelectric contact, and a flexible piezoelectric material with an active area of 4 cm x 4 cm. Secondly, a finite element model (FEM) was developed for the hybrid devices using COMSOL Multiphysics, to understand the coupling between both effects, study the load resistance matching and parameter optimization in order to find higher output performance.

Thirdly, the generated output voltage, output current, transferred charges and output power by the proposed hybrid devices were characterized in water conditions using a breaking water wave generator tank, which simulates the conditions of the mechanical energy generated by ocean wave impacts on the shoreline at low frequencies mentioned above. The output performance of the hybrid prototypes was compared with triboelectric nanogenerators and piezoelectric nanogenerators (PENG) tested in similar conditions [13, 14]. Additionally, a load resistance matching experiment was performed with the objective being to obtain maximum output power performance from the prototypes.

Finally, the ability to charge a variety of capacitors with a single hybrid device, and a grid of four hybrid devices connected in parallel [24-26] was characterized. An enhancement in the output performance by exploiting the advantage by the combined triboelectric-piezoelectric effects using the proposed grid of energy harvesters was achieved as a result of simultaneous operation of both mechanisms under water wave impact at low frequency range in a single contacted-pressed-release operation. Additionally, it was demonstrated that such grid of energy harvesters has the potential to drive small electronic devices that will enable future advancement for powering a variety of battery-less, self-powered marine sensing platforms for environmental monitoring.

2. Working mechanism of electricity generation using triboelectric-piezoelectric effects under water wave impact

The three-electrode structure of the hybrid nanogenerator prototypes utilizes an arc-shaped dielectric-to-conductor triboelectric contact and a flexible piezoelectric material with an active area of 4 cm x 4 cm (Fig. 1 a, Fig. 1 e and Fig. 1 f). The energy applied to the hybrid nanogenerator system is translated into two coupled effects. The triboelectric effect is affected by $E_{kinetic}$ (1), which is the energy carried by the moveable arc-shaped dielectric layer that plays the role of contact material for triboelectricity, and $E_{elastic}$ (2) which is the energy stored in the dielectric layer acting as a spring for separation after contact.

$$E_{kinetic} = \frac{1}{2}mv^2 \tag{1}$$

$$E_{elastic} = \frac{1}{2}k_t x^2 N \tag{2}$$

where, v is the average velocity of the dielectric layer when the contact is made, caused by the water wave impact, m is the mass of the moveable arc-shaped layer. k_t is the spring constant due a flexural stiffness, x is the displacement of the arc-shaped layer that is equal to the spacing between the two contacting surfaces (x = 5 mm), and N is the number of springs considered for the arc-shaped structure of the hybrid nanogenerator (N = 2).

Additionally, the piezoelectric effect is affected by the mechanical energy of the water wave impact which stress the piezo-layer a distance a, and that can be approximately calculated by the work done, W due to pressing/pulling as shown in (3)[27].

$$W = F\Delta L \cong \sigma A_c \frac{2a^2}{L_0} \tag{3}$$

The piezo-film is stressed by tension $F = \sigma A_c$, where σ is tensile stresses, and A_c is the cross-sectional area of the piezoelectric layer. Considering the piezo-layer as an elastic medium, the spring constant k_p due the stiffness in stretching that is given by $k_p = EA_c/L_0$, where E is the Young's modulus. The length change of the piezoelectric material ΔL, can be approximated as ΔL

$\cong \frac{2a^2}{L_0}$, defining $L \cong L_0$ [27].

The operation of the PENG (Fig. 1 b) and the two-electrode structures of the arc-shaped TENG (Fig. 1 c) and DMCS-TENG with self-restoring structure (Fig. 1 d) used to compare the output performance of the hybrid nanogenerator under breaking wave impact is illustrated in the Supplementary Information document.

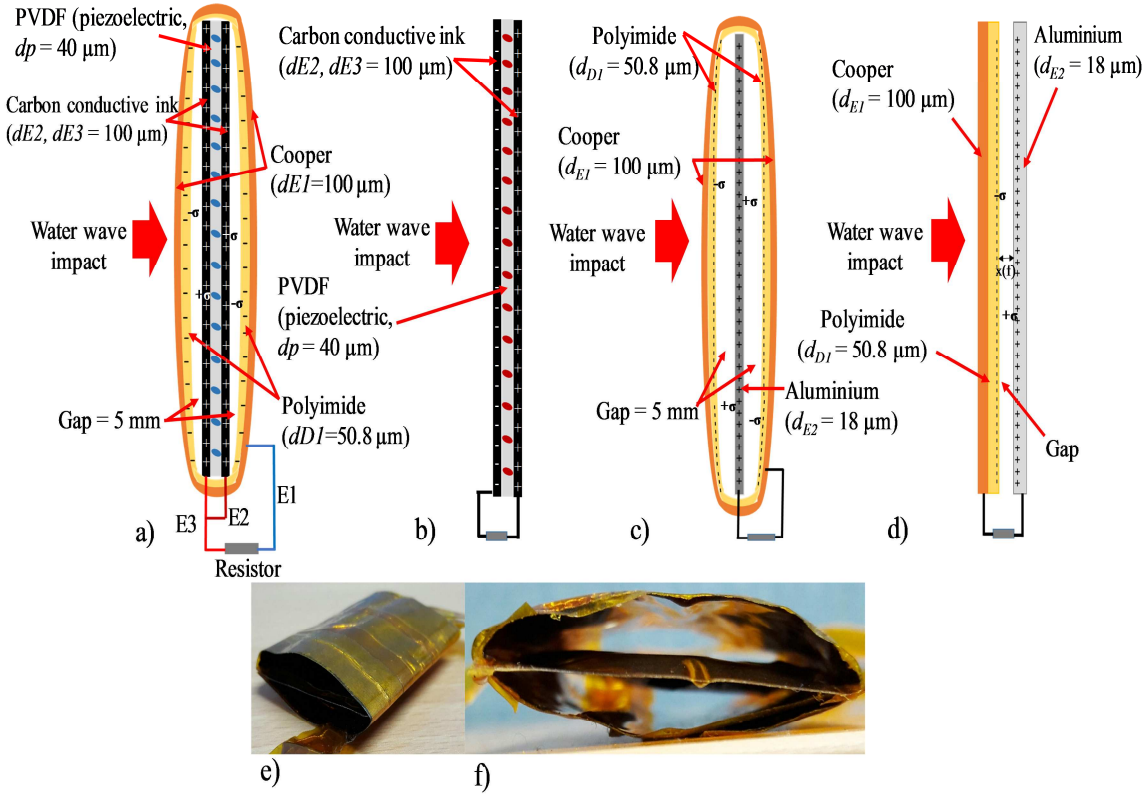

Fig. 1. Two-dimensional schematic of the a) Hybrid nanogenerator, b) PENG with charge distribution when it is under an external force. c) The arc-shaped DMCS-TENG, and d) the DMCS-TENG self-resetting system. e) Digital photo and f) cross sectional digital photo of the hybrid nanogenerator.

The simultaneous operation of triboelectric-piezoelectric effects under water wave impact is depicted in Fig. 2 (a-e). Before the water wave impacts the hybrid nanogenerator, there are accumulated negative charges in the dielectric layer, and positive accumulated charges in electrode 2 (E2) and electrode 3 (E3) caused by dielectric-to-conductor triboelectrification after few cycles of movement (Fig. 2 a and Fig. 2 f). First, the impact of the water wave produces forward triboelectric effect as the gap between contact-layers decreases, and a piezoelectric effect as the charges flow due to tensile stress on the piezoelectric layer (Fig. 2 b and Fig. 2 g). The piezoelectric polarization influences the charge distribution on electrode 1 (E1), and E3 since they are connected. Positive charges flow to E3 leaving E1 with negative charges, when the device is contacted and pressed (Fig. 2 b and Fig. 2 g). Second, as the water wave breaks down and moves off the hybrid device, no polarization exist so E1 and E3 remain electrically neutral as the device it is in the “contacted and released” state (Fig. 2 c and Fig. 2 h). Third, the gap increases and hence this changes the electric field between the contacted dielectric-conductor materials. The piezoelectric material recovers to its original shape, with a change in piezoelectric potential and electric field, driving the charges in the load to flow in an opposite direction. Therefore, there are charges with opposite signs in E1 and E3, respectively (Fig. 2 d and Fig. 2 i) as the structure of the hybrid prototype is releasing. Finally, the hybrid nanogenerator is fully released, and reaches equilibrium once again (Fig. 2 e). Thus, one operational cycle of the hybrid prototype is achieved. Once the following water wave impacts the hybrid prototype, a periodic output will be obtained (Fig. 2 a-e).

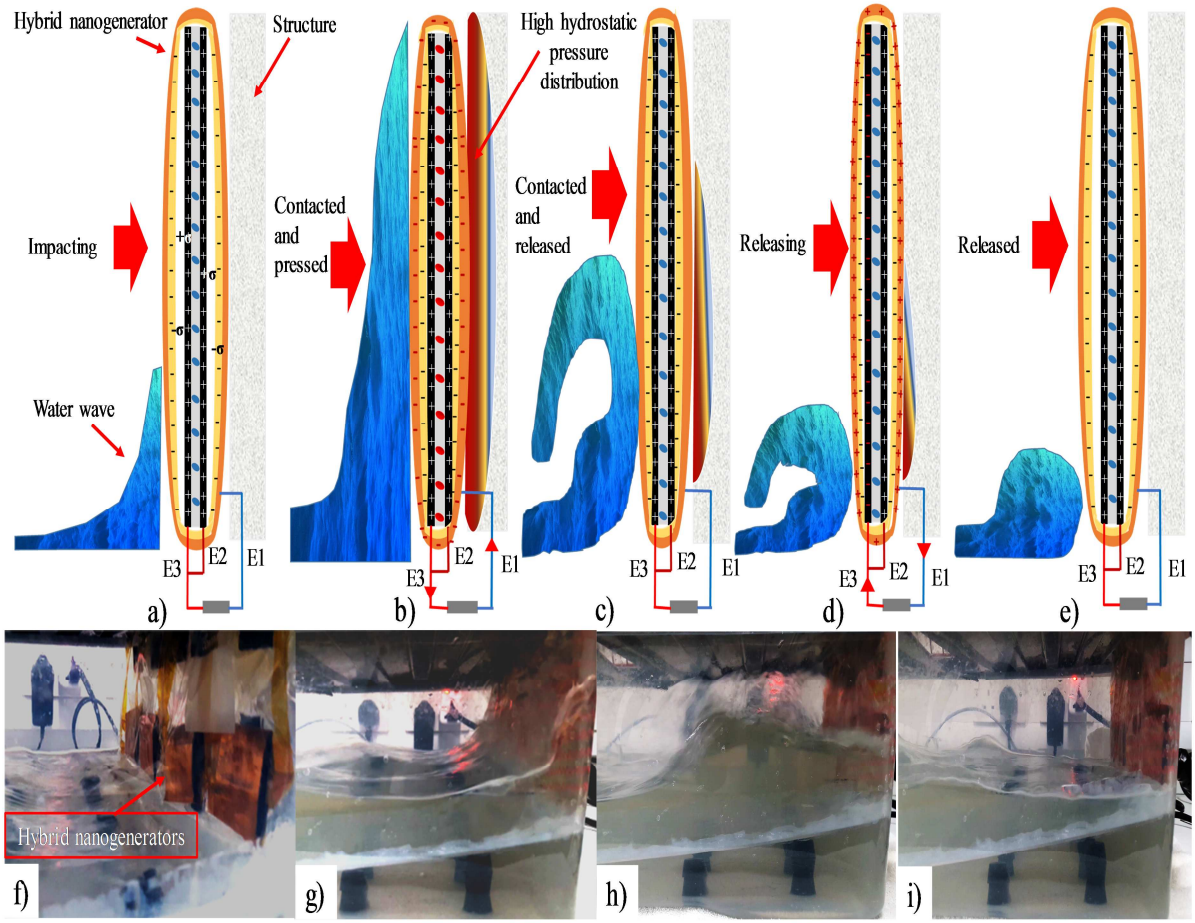

Fig. 2. (a-e) Working mechanism of the hybrid nanogenerator with a simultaneous operation and electricity generation of triboelectric-piezoelectric effects under water wave impact. Digital photos of grid of hybrid nanogenerators in the breaking wave impact generator tank f) before receiving water wave impact, g) contacted and pressed, h) contacted and released, and i) releasing.

3. Hybrid nanogenerators FEM

An FEM was developed for the hybrid energy harvesters in order to understand the output performance, load resistance matching of simultaneous coupling between triboelectric and piezoelectric effects under water wave impact. We first consider the "*V*-*Q*-*x* relationship" [28, 29] proposed for modelling the operating principles of a TENG. When it is connected with an external resistive load (R_l), the maximum output power of the whole system can be derived using Kirchoff's law [28, 29]:

$$R_t \frac{dQ}{dt} = -\frac{1}{C(x)}\mathrm{Q} + V_{OC(x)} = -\frac{1}{C}Q + V_{OC} \qquad (4)$$

where *Voc* is the voltage generated between two DMCS-TENG contacts, *Q* is the amount of charge within the two contacts, *C* is the capacitance of the two electrodes, and *x* is the distance between the triboelectric layers that varies with the mechanical energy and phase of motion at time, t. According to this model, the output power performance by the DMCS-TENG depends on the output current (*I*). The voltage (*V*) is influenced by the load resistance, and the surface charge density σ depends on the properties of the materials in contact. The piezoelectric nanogenerator has a smaller output voltage but larger output current, which is caused by the relatively low equivalent resistance. The equivalent external resistance of a piezoelectric nanogenerator (R_p), when the output power reaches its maximum value can be expressed as [30]:

$$R_p = \frac{d}{bL\varepsilon_p f} \quad (5)$$

where d_p, b, L and ε_p are the thickness, width, length and permittivity of the piezoelectric material and f is the frequency of the external mechanical energy.

The FEM simulations were performed by coupling solid mechanics, electrostatics and electrical circuit interfaces so as to model the output current, voltage and power generated by the hybrid nanogenerators connected to resistive loads (varying from 0.001 to 100 MΩ) under a horizontal applied periodic motion at the oscillating frequencies of 0.7, 1.2, 1.8, 2.5 and 3 Hz. This applying a waveform, input, and a boundary load on the hybrid device as described in TABLE I. The model is based on the hybrid prototype structure as shown in Fig. 1 a, with different lengths of (L = 4 cm. 6 cm and 8 cm), so that the best design can be found. The device structure includes a PVDF piezoelectric layer (d_p = 40 µm) with a piezoelectric polarization ($x1$) of 150 µC/m^2 that is connected to two silver electrodes ($d_{E2,}$ d_{E3} = 10 µm) E2 (grounded) and E3. A copper E1 (d_{E1} = 10 µm) with a polyimide dielectric layer (d_{D1} = 50.8 µm) acts as the triboelectric part. The two tribo-charge surfaces were assigned with the theoretical maximum surface charge density [13, 31] σ_{max} = ±34.063 µC/m^2, respectively (TABLE I).

TABLE I
PARAMETERS USED IN THE FEM

Parameter	Value
R_load (R_L)	0.001 to 100 MΩ
R_TENG (R_t)	10 MΩ
R_PENG (R_p)	0.5 MΩ
Frequencies (f)	0.7, 1.2, 1.8, 2.5, and 3 Hz
Time (t)	1 s
Waveform	6*pi*f
Input	wv1(t)
Boundary load	solid.rho*g_const
Surface charge density (σ_{max})	±34.063 µC/m^2
Piezoelectric polarization (x_1)	150 µC/m^2
Time dependant (Simulation time)	range(0,0.006,0.72)s
Dielectric layer (Polyimide, d_{D1})	Thickness = 50.8 µm
	Length = 4, 6 and 8 cm
Piezoelectric layer (PVDF, d_p)	Thickness = 40 µm
	Length = 4, 6 and 8 cm
Copper electrodes (d_{E1})	Thickness = 10 µm
	Length = 4, 6 and 8 cm
Silver electrodes (d_{E2}, d_{E3})	Thickness = 10 µm
	Length = 4, 6 and 8 cm
Gap	150 µm

A series of simulations were performed in order to analyse the output performance of the entire system at the frequency range aforementioned. First, an analysis of the load resistance influence in the output performance and electric potential of triboelectric and piezoelectric part was performed independently as illustrated in Fig. 3 a and Fig. 3 b. The results show a highest output power performance with the structures of L = 8 cm at the oscillation of 3 Hz. The triboelectric nanogenerator and piezoelectric nanogenerator reached the maximum output power of 21.88 mW and 19.56 mW with a 10 MΩ and 0.5 MΩ load, respectively (Fig. 3 d).

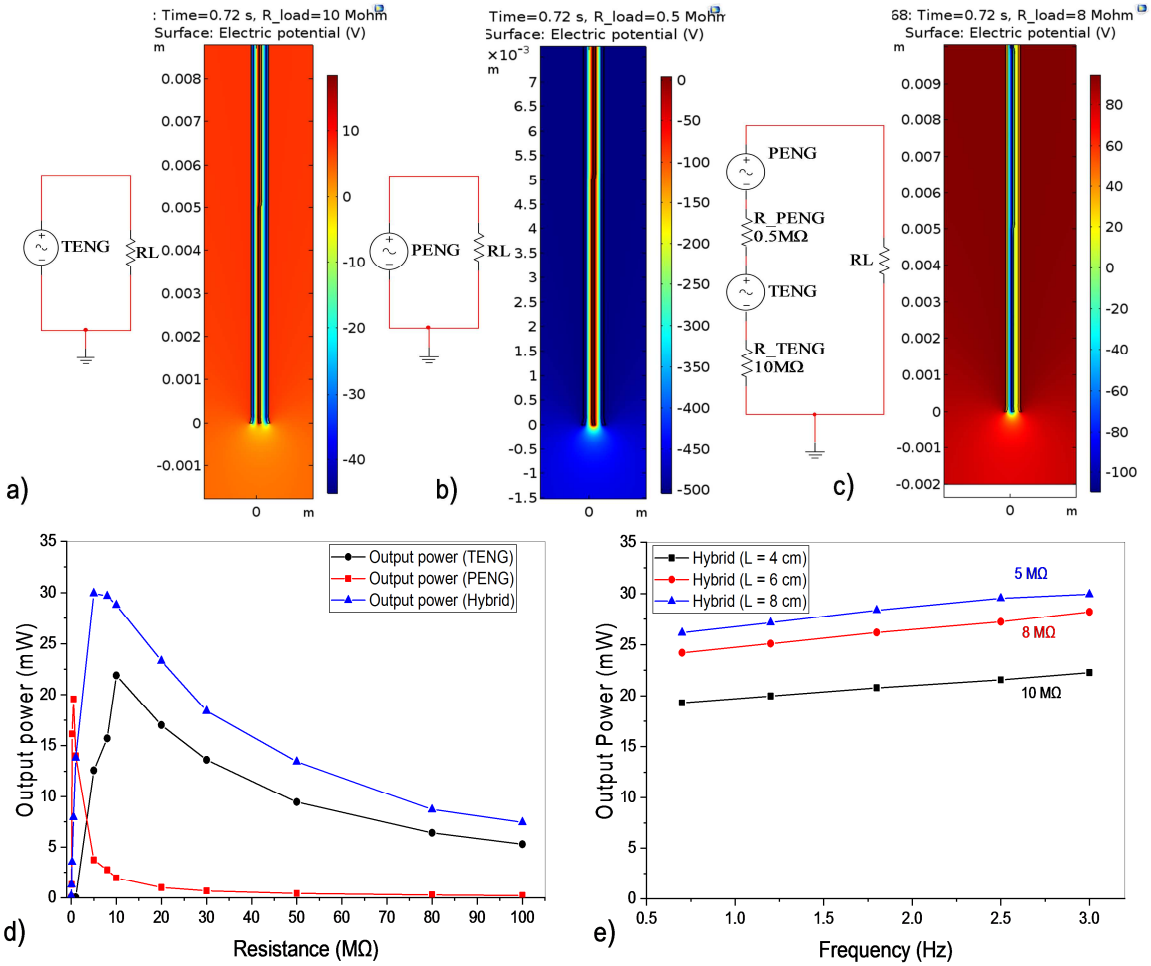

Fig. 3. Electric potential model and simulated electric circuit diagram of a) TENG, b) PENG, and c) simultaneous coupling of triboelectric-piezoelectric effects (hybrid nano generator). d) Simulation of the influence of the load resistance in the output power of TENG, PENG and Hybrid prototype. e) Output power of the simulated hybrid devices with different lengths (3 cm, 6 cm and 8 cm) under different frequencies (0.7 Hz to 3 Hz) that highlights the optimum load resistance for every structure.

Therefore, the coupling of both effects was performed using the electric circuit diagram shown in Fig. 3 c, to perform a quantitative load matching analysis of the hybrid device output performance, and electric potential. The output power of the hybrid prototype shows an enhancement by a factor of 1.36 and 1.56 compared with the simulated triboelectric nanogenerators and piezoelectric nanogenerators tested in similar conditions respectively (Fig. 3 d). The maximum generated output voltage 381.89 V and output current of 76.87 μA, which corresponds to the maximum output power of 29.94 mW, with a 5 MΩ load as shown in Fig. 3 d, and Fig. 3 c illustrates the electric potential generated by the hybrid prototype.

Additionally, the increase in the length (L = 8 cm) and oscillating frequency (0.7 Hz to 3 Hz) of the hybrid devices promote an increase in the output power by a factor of 1.34 (L = 4 cm) and 1.06 (L = 6 cm), respectively. Consequently, the optimum load resistance reduces as response

[28], so for the hybrid structures L = 4 cm and L = 6 cm the optimum resistances were 10 MΩ and 8 MΩ (Fig. 3 e), with a maximum output power of 22.27 Mw, and 28.22 mW, respectively (see Supplementary Information document).

Although the structure of 8 cm x 8 cm is the best to obtain higher output performance for the hybrid device, the structure with the active area of 4 cm x 4 cm was selected to fabricate the hybrid nanogenerator, with the purpose of obtain a stable output performance operation. This when the hybrid device and the grid of 4 hybrid devices were attached into the operation area (13 cm x 34 cm) in the water wave impact generator tank (52 cm x 34 cm x 18 cm).

4. **Hybrid nanogenerator prototype fabrication and electrical characterization set-up**

4.1 Fabrication

The hybrid prototypes composed with a three-electrode configuration with an active area of 4 cm x 4 cm depicted in Fig. 1 a and Fig 1 e-f, were fabricated using a simple and low-cost process. Two carbon conductive ink electrodes (E2 and E3) were manually printed on both sides of a flexible PVDF piezoelectric layer (PIEZOTECH, d_p = 40 µm) at room temperature (Fig. 1 b). Therefore, by using suitable triboelectric materials [13, 18-20], a dielectric polyimide (d_{D1} = 50.8 µm) was manually fixed with conductive glue at room temperature on a copper layer (d_{E1} = 100 µm) which acts as E1. Additionally, the E1 layer was manually insulated on the other side using Kapton polyimide heat and chemical resistant tape at room temperature. Then, the E1 layer was placed facing the polyimide dielectric layer over the piezoelectric layer and bonded using Kapton tape at room temperature to form the arc-shaped dielectric-to-conductor structure with a gap of 5 mm on both sides (Fig. 1 a).

Additionally, the arc-shaped TENG have an active area of 4 cm x 4 cm (Fig. 1 c), and an acrylic sheet was selected as a substrate material. An aluminum conductor layer (thickness = 18 µm) was attached to the acrylic with a thin adhesive layer, at room temperature. Acting as both the triboelectric material and the electrode that is grounded. The polyimide dielectric layer (thickness = 50.8 µm) was fixed with an arc-shaped form using conductive acrylic adhesive at room temperature on a copper layer (thickness = 100 µm) that is used as the second electrode connected to an external load for electrical characterization. Additionally, the copper layer was manually insulated on the other side using Kapton. The maximum gap between the arc-shaped dielectric layer and the conductor layer is 5 mm. Therefore, the DMCS-TENG with self-restoring structure was fabricated following the process described in [13] using the dielectric-metal contact between polyimide and aluminium (Fig. 1 d).

4.2 Electrical characterization

The electrodes of the fabricated hybrid prototype were connected to two full wave bridge rectifiers in order to perform the electrical characterization, as depicted in Fig 4 a. E1, and E3 were connected to each rectifier as a supply from the hybrid device in a simultaneous operation using the triboelectric effect and piezoelectric effect, respectively. E2 was connected in both rectifiers that is used as the second triboelectric material (grounded) and second electrode (grounded) of the piezoelectric layer.

Their output voltage, output current, transferred charges and output power performance was compared with triboelectric nanogenerators, and piezoelectric nanogenerators [13] (Fig. 1 b-d) which were characterized in similar water conditions. The energy harvesters were insulated with polyethylene packaging, in order to protect them from the contact with water. Such devices were placed at the wall on the right side of the tank facing the impact of the water wave as shown in Fig. 4 b, where the water wave breaks with an amplitude of 10 to 12 cm and frequencies of 0.7 Hz to 3 Hz [13, 14]. A practical load resistance matching analysis (varying between 100 Ω to 100 MΩ) to reach a maximum output power performance with the hybrid nanogenerators was performed.

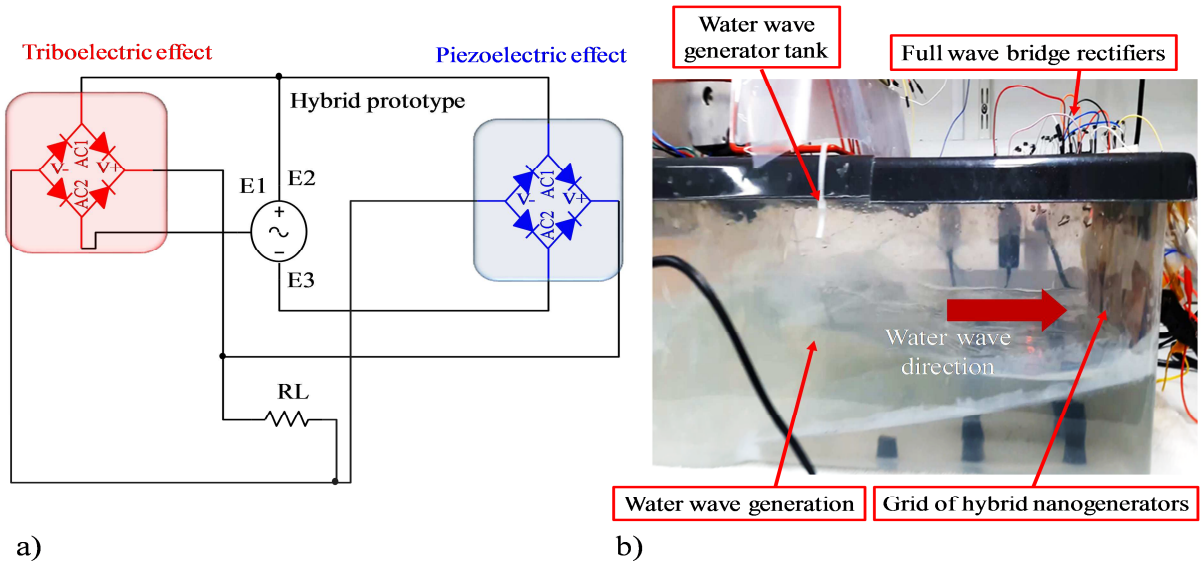

Fig. 4. a) Circuit diagram of the hybrid nanogenerators for the load matching and capacitor charging experiments. b) Grid of hybrid nanogenerators placed in the water wave generator tank for its output performance measurements.

Consequently, the ability to charge a variety of capacitors (between 2.2 to 100 µF) for a period of 80 seconds with a single hybrid device, piezoelectric device, triboelectric devices and a grid of four hybrid devices (connected in parallel in order to increase their output performance) was tested. Furthermore, a durability test was performed to the hybrid devices under water wave impact during different periods between 30 min to 180 min and number cycles of operation (see Supplementary Information document). Moreover, the potential of the grid of hybrid devices to charge and discharge capacitors was tested for a longer period. The output power generated of the energy harvesters was derived using the rectified output current and rectified output voltage measurements performed using an Agilent Technologies N6705B power analyser. The transferred charges was measured with an electrometer Keithley 6514 (See Supplementary Information document), and the charging performance of the hybrid devices was measured with a digital oscilloscope Tektronix TDS 2014C, respectively (10 measurements performed on each sample).

5. Experimental results and discussion

The rectified output current, voltage and charge transferred of the hybrid, TENG and PENG prototypes increases linearly, as the frequency (0.7 Hz – 3 Hz) and amplitude (10 cm – 12 cm) of breaking wave impact rises (Fig. 5 a-l). The maximum output current, voltage and transferred charges generated for the hybrid nanogenerator increases from ~35.7 µA to ~140.93 µA, ~68.23 V to ~229.31 V, and ~102.12 nC to ~399.29 nC, (Fig. 5 a-c) respectively. Thus, the maximum output power performance increases from ~6.79 mW to 16.94 mW. The power performance of the hybrid prototypes shows an enhancement by a factor of 2.24, 4.80 and 3.21 compared with the arc-shaped TENG, DMCS-TENG and the piezoelectric nanogenerator (Fig. 6 a). Such output current, voltage and charge transferred increases linearly from ~6.28 µA to ~76.52 µA, ~34.02 V to ~107.89 V, and ~17.73 nC to ~292.90 nC (Fig. 5 d-l). Accordingly, the maximum output power performance of those energy harvesters were between ~0.87 mW to ~11.42 mW (Fig. 6 a), tested in similar conditions of the mechanical energy generated by water wave impacts, and connected to a 1 MΩ load resistance, respectively. Furthermore, the enhancement was verified with the charging performance of the energy harvesters charging a capacitor of 2.2 µF for 80 seconds, where the hybrid nanogenerators reached a maximum voltage of 5.4 V as shown in Fig. 6 b.

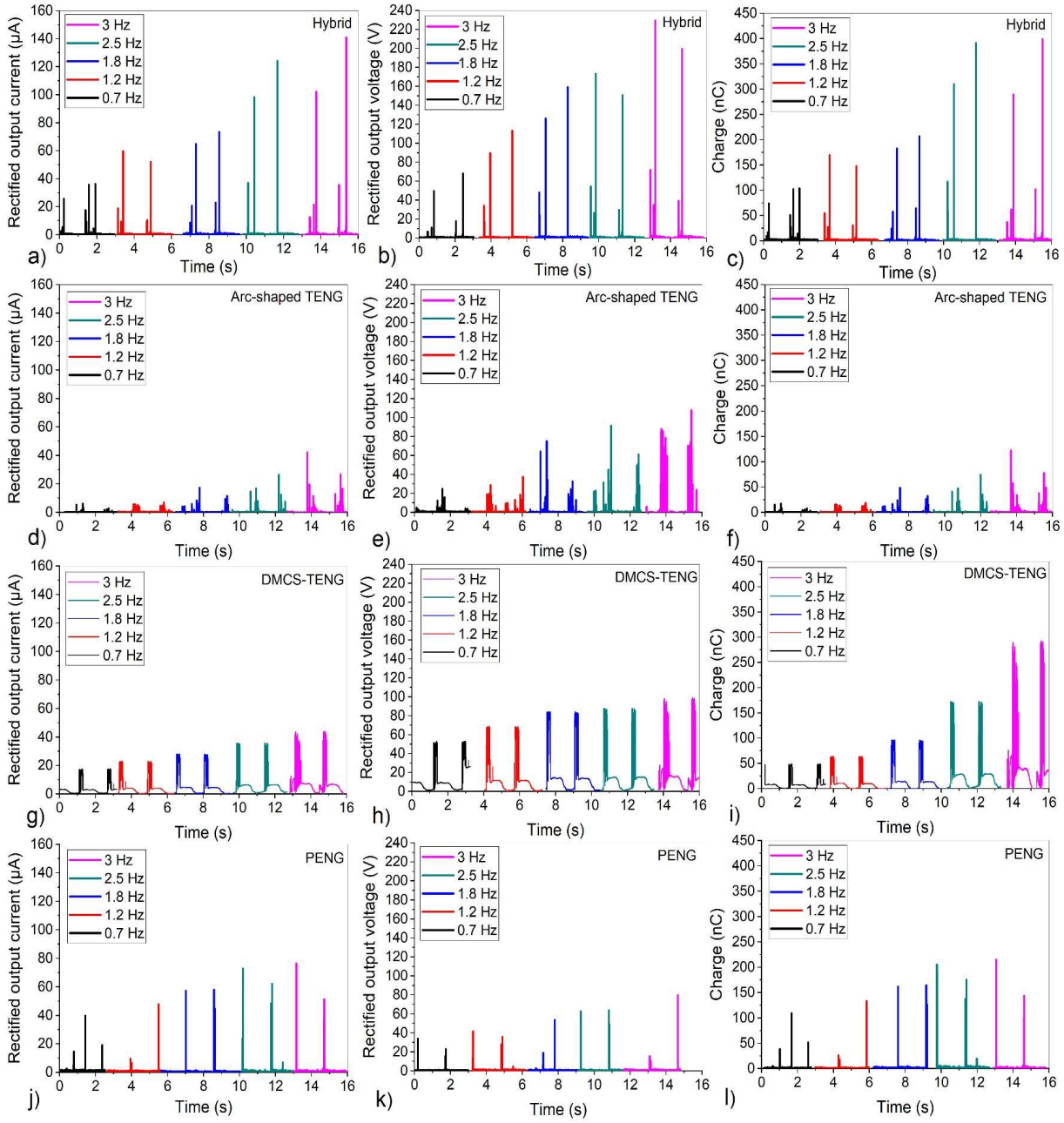

Fig. 5. a) Average rectified instantaneous output current, b) output voltage, and c) transferred charges of hybrid nanogenerator. In comparison with (d-f) arc-shaped TENG, (g-i) DMCS-TENG, and (j-l) PENG average rectified instantaneous output current, output voltage, and transferred charges connected to a 1 MΩ load resistor tested in a water wave impact generator tank under different frequencies of impact between 0.7 Hz to 3 Hz.

Furthermore, the maximum average output power and power density of ~15.92 mW and ~0.99 mW/cm^2, respectively was generated with a load resistance of 8 MΩ through the load resistance matching practical experiment (Fig. 6 e). This is compared with the maximum generated output power of ~19.76 mW with a load resistance of 10 MΩ reached through the simulated model of the hybrid prototypes (L= 4 cm) (see Supplementary Information document). Such output performance difference results from assuming the maximum surface charge density between the triboelectric materials in contact, and piezoelectric polarization under ideal conditions.

Additionally, the maximum voltage reached by the grid of hybrid devices was 12.87 V, compared with a single unit that reached a maximum value of 5.4 V charging a capacitor of 2.2 μF for 80 seconds as depicted in Fig. 7 a, and Fig. 7 b. The grid of hybrid devices connected in parallel with a total active area of 256 cm^2 resulted in an enhancement factor of 2.43 in the output

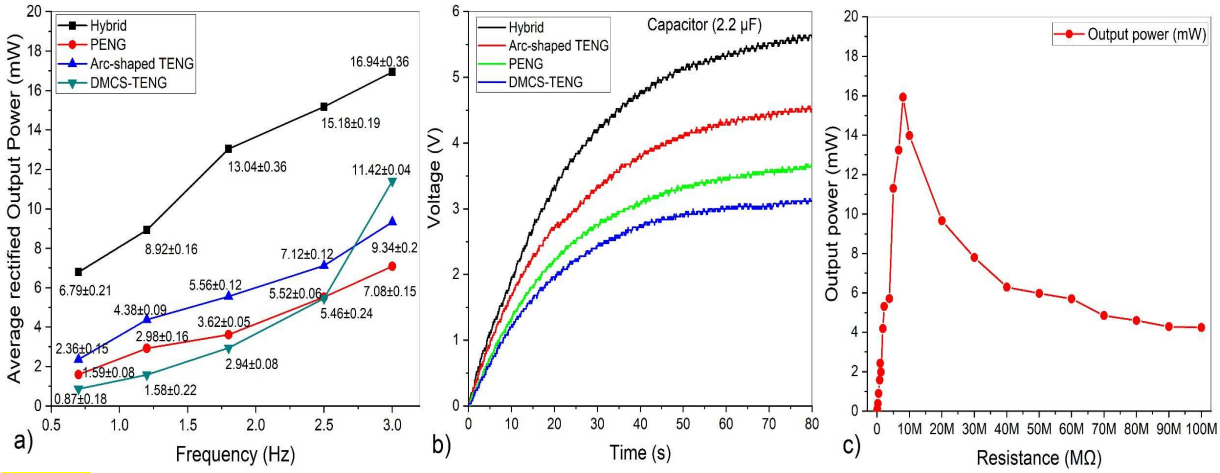

Fig. 6. a) Rectified average instantaneous output power and its standard deviation analysis calculated (10 measurements performed for each sample) of Hybrid device compared with TENG and PENG devices connected to a 1 MΩ resistor under water wave impact (0.7 Hz to 3 Hz). b) Charging performance of a single hybrid device, arc-shaped TENG, PENG, and DMCS TENG connected to a 2.2 µF capacitor. c) Load resistance matching analysis to reach the highest output power performance of the 4 hybrid devices tested in the water generator tank.

power (Fig. 7 f) and output performance enhancement in charging different capacitors compared with a single hybrid nanogenerator. Such a grid of four energy harvesters generated a maximum average instantaneous output current, voltage and charge transferred, which rises steadily under the different frequencies (0.7 Hz to 3 Hz) from ~89.05 µA to ~314.13 µA, ~185 V to ~631 V, and ~346.38 nC to ~1095.62 nC, (Fig. 7 c-e) respectively. As a result, the maximum generated output power and power density were between ~10.70 mW to ~46.58 mW, and ~0.042 mW/m^2 to ~ 0.18 mW/m^2 with a load resistance of 8 MΩ, respectively as depicted in Fig. 7 f. Furthermore, to calculate the average energy conversion efficiency (ECE) η of the grid of hybrid device system, defined as the ratio between the electric energy ($E_{electric}$) delivered to the load resistor of 8 MΩ and the mechanical energy ($E_{waterwave}$) applied by the water wave impact over a period (t) of 30 seconds with the different frequencies. The $E_{electric}$ released by the grid of hybrid nanogenerators was

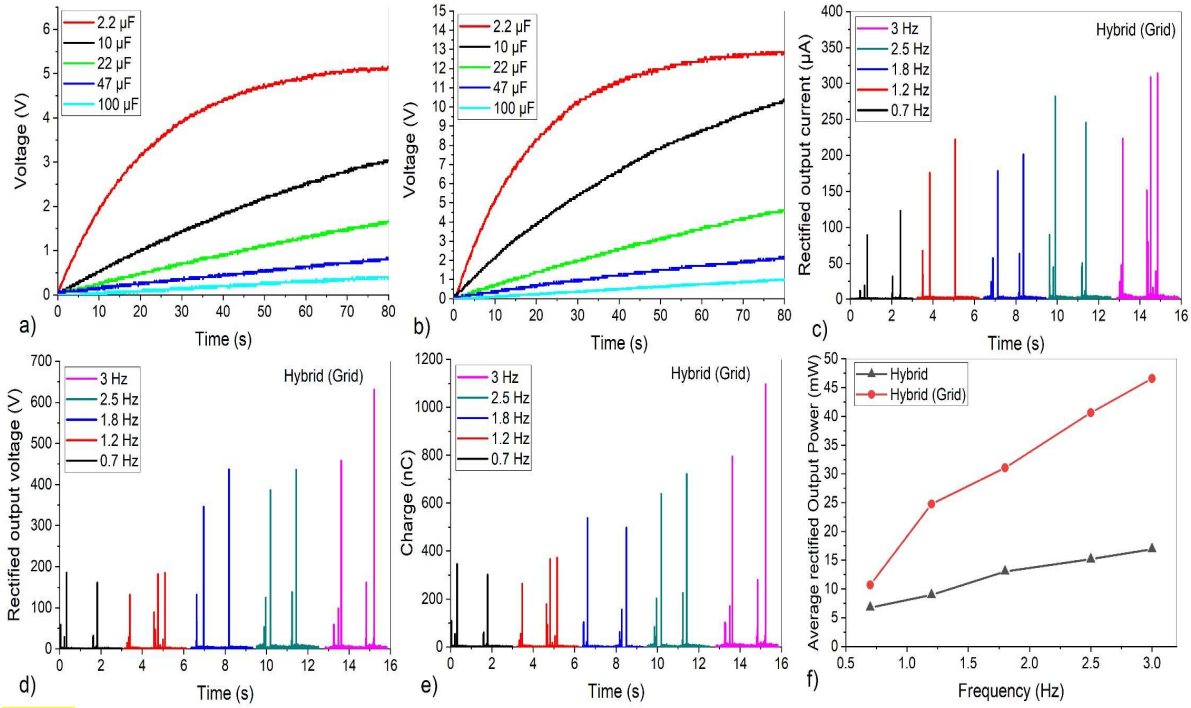

Fig. 7. a) Charging performance of a single hybrid device, and b) a grid of 4 hybrid devices connected in parallel to different capacitors (2.2 µF – 100 µF). c) Rectified instantaneous output current, d) output voltage, e) transferred charges, and f) output power of a grid of hybrid devices compared with a single hybrid device unit connected to a 1 MΩ load resistor

calculated by:

$$E_{electric} = \int_{t1}^{t2} RI^2 dt = 16.10\,J \quad (6)$$

where I is the average instantaneous current and R is the load resistance. The total average energy (potential energy and kinetic energy) produced by the water wave generator tank was calculated as [32]:

$$E_{waterwave} = \frac{1}{2}\rho g A^2 = 59.36\ \text{J} \quad (7)$$

where g is the acceleration of gravity (g = 9.8 m/s^2), ρ is the density of water (ρ = 1000 kg/m^3), and A is the wave amplitude (between ~10 cm to ~12 cm, frequencies = 0.7 Hz to 3 Hz). Consequently, the overall η of the grid of hybrid devices was 27.12% calculated by [33]:

$$\eta = \frac{E_{electric}}{E_{waterwave}} x100\% = 27.12\% \quad (8)$$

Moreover, due to the improvement of the water wave impact energy harvesting, and good performance storing energy in different capacitors using the grid of hybrid nanogenerators, an application was demonstrated.

The grid of hybrid nanogenerators was used to power a one way wireless 433 MHz transmitter (Seeed 113990010) and sent a signal to the receiver to turn on 4 Kingbright L-7104PWC-A 3 mm white LEDs (1200 mcd), with a transmission distance from 2 m to 8 m as shown in Fig. 8 a and Fig. 8 b. This was achieved after charging a capacitor of 47 µF between 312 seconds to 857 seconds, the voltage reached was within 2.95 V to 8.51 V and the switch was open to power up the

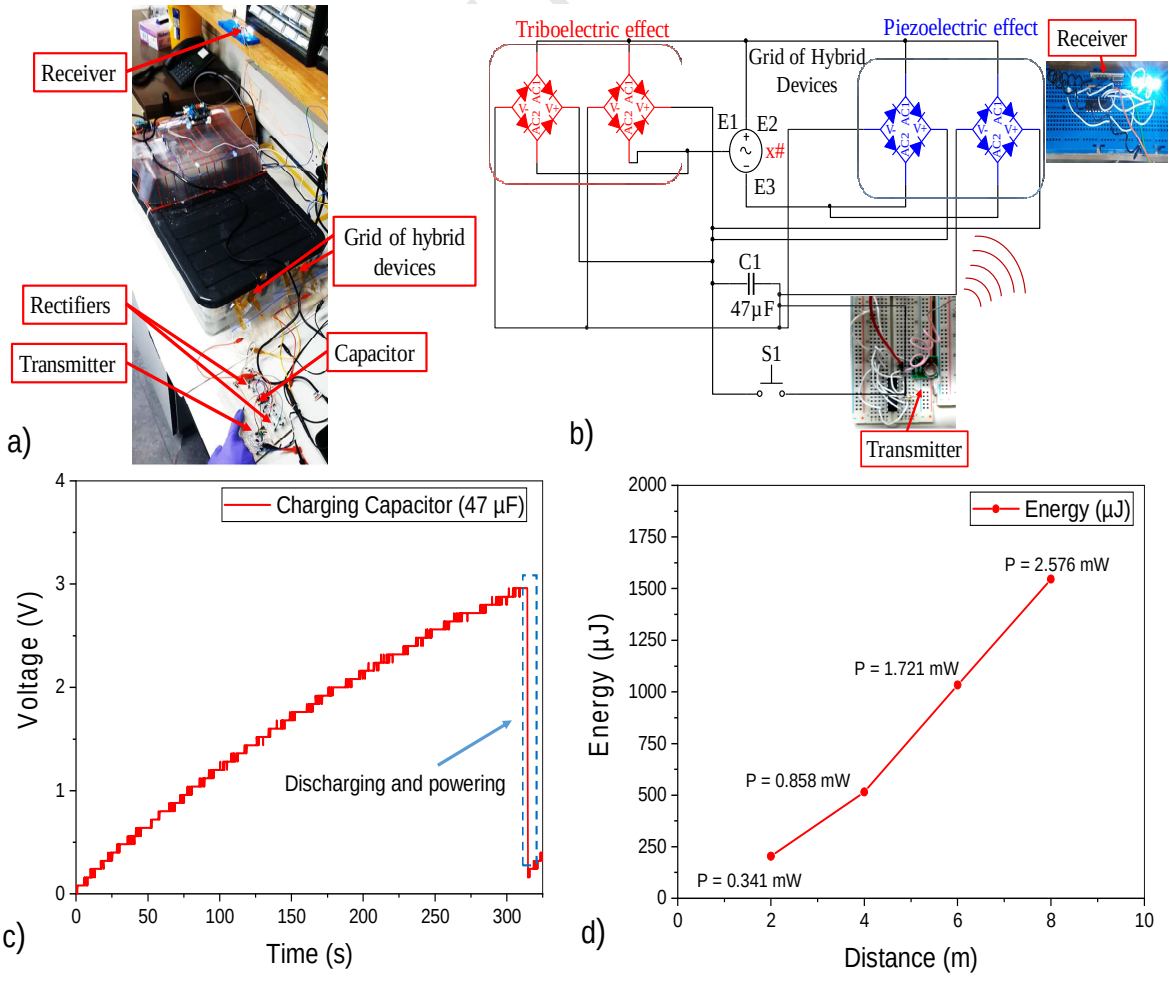

Fig. 8. a) Set-up for powering the wireless transmitter with the grid of hybrid nanogenerators under the water wave impact. b) Electrical circuit diagram of the hybrid nanogenerators to charge the 47 µF capacitor for powering the wireless transmitter. c) Capacitor charging and discharging process for powering the wireless transmitter under the water wave impact with a frequency of 1.2 Hz. d) Energy stored in the 47 µF capacitor for the grid of hybrid devices, and the power generated for the capacitor during the discharging process for powering the wireless transmitter to send a signal to a receiver with a transmission distance from 2 m to 8 m.

transmitter as depicted in Fig. 8 c. Furthermore, as the transmission distance increases, more energy was required with a longer charging time required for the capacitor. The energy stored in the capacitor for the grid of hybrid devices, and the power generated for the capacitor during the discharging process for powering the wireless transmitter were between 204.51 µJ to 1.54 mJ, and 340.85 µW to 2.57 mW, respectively (Fig. 8 d). Besides, it was demonstrated that the grid of hybrid energy harvesters show the capacity to drive small electronic devices by the achieved output power levels (see Supplementary Video S1).

Finally, we consider the scale up the capability of a grid of these hybrid energy harvesters by constructing large water-hybrid nanogenerators-structure interfaces (Fig. 9) with an area of 18 m^2 that receives wave sizes among 0.3 m to 4 m [34]. If the interface is integrated with 11,250 hybrid devices connected in parallel, it is estimated to generate an average output power, and energy of ~21.61 W, and ~23.70 kJ. Considering a water wave impact over the proposed interface with a maximum amplitude of 4 m, it is calculated to generate a total energy of 78.4 kJ using (7). Using (8), it is calculated that the large-scale hybrid nanogenerators could have an energy conversion efficiency of 30.22 %, harvesting the impact energy of water waves in large scale.

As a result, with the enhancement of the water wave impact energy harvesting performance, the grid of hybrid nanogenerators is suitable for powering a variety of battery-less systems as wireless nodes for coastal sensing applications.

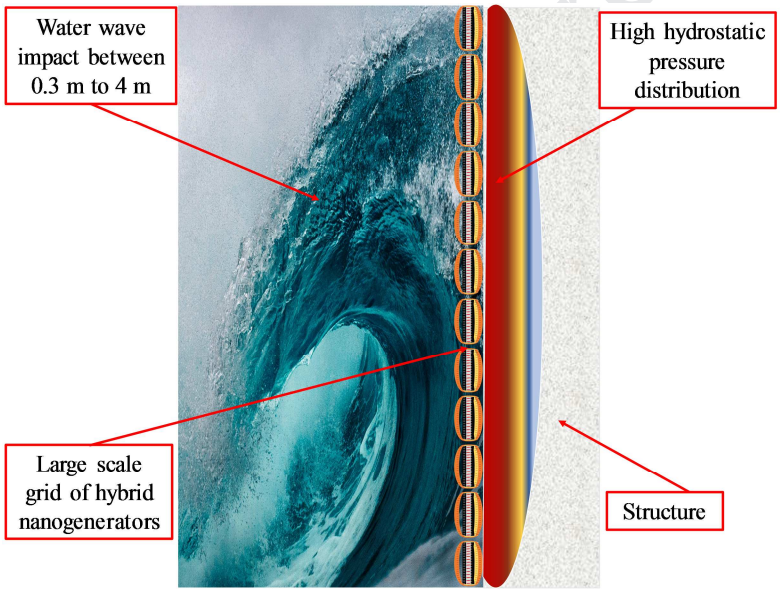

Fig. 9. Two-dimensional schematic illustration of the configuration of the proposed large water-hybrid nanogenerators-structure interfaces to escalate the energy harvesting of water wave impact (Ocean water wave adapted from [35]).

6. Conclusion

In this study, the improvement in the output performance of prototype devices for ocean wave, impact force energy harvesting was achieved by simultaneously coupling triboelectric-piezoelectric effects, and also by the attribution of an electrical parallel connection of a grid of such devices. This was verified by measuring the output current, voltage, charge transferred, output power, and examining the ability to charge a selection of capacitors with a grid of four hybrid devices connected in parallel and tested under simulated wave conditions at low frequencies. As a result the output performance response of the hybrid devices increases linearly, as the frequency between 0.7 Hz to 3 Hz and amplitude between 10 cm to 12 cm of breaking wave impact rises. Moreover, the grid of hybrid nanogenerators has the potential to drive low-power electronic devices. This was demonstrated by using the stored energy in a capacitor charged over different periods of time. The devices were capable of powering a wireless transmitter and sending a signal to a receiver at varying distances. Finally, the high output power obtained, shows that the

integrated grid of devices offers a promising innovative approach for the production of high-performance energy harvesting mechanisms focused on harvesting water wave impact energy. These are capable of energizing self-powered marine sensing systems for environmental monitoring requiring an average power consumption in the range from 1 mW to 100 mW [36, 37]. Further, it is estimated that with the construction of large water-hybrid nanogenerator-structure interfaces for the generation of electricity on a larger scale, harvesting the impact of the water waves for powering networks of self-powered sensing systems for smart fish farms having an average power consumption from 100 W to 1 kW [38]. This research work provides a promising alternative approach to harvest breaking water wave impact energy that contributes to the previous blue energy harvesting studies, which are focused on harvesting shallow water wave energy [2-10].

Acknowledgements

The authors thank CONACYT for the fellowship awarded to Ulises Tronco Jurado.

References

[1] N. Elvin and A. Erturk, *Advances in energy harvesting methods*. New York Heidelberg Dordrecht London: Springer 2013.

[2] T. X. Xiao, X. Liang, T. Jiang, L. Xu, J. J. Shao, J. H. Nie, *et al.*, "Spherical triboelectric nanogenerators based on spring□assisted multilayered structure for efficient water wave energy harvesting," *Advanced Functional Materials*, vol. 28, p. 1802634, 2018.

[3] X. Li, J. Tao, X. Wang, J. Zhu, C. Pan, and Z. L. Wang, "Networks of high performance triboelectric nanogenerators based on liquid–solid interface contact electrification for harvesting low□frequency blue energy," *Advanced Energy Materials*, vol. 8, p. 1800705, 2018.

[4] X. Zhang, M. Yu, Z. Ma, H. Ouyang, Y. Zou, S. L. Zhang, *et al.*, "Self□Powered Distributed Water Level Sensors Based on Liquid–Solid Triboelectric Nanogenerators for Ship Draft Detecting," *Advanced Functional Materials*, vol. 29, p. 1900327, 2019.

[5] M. Xu, T. Zhao, C. Wang, S. L. Zhang, Z. Li, X. Pan, *et al.*, "High power density tower-like triboelectric nanogenerator for harvesting arbitrary directional water wave energy," *ACS nano*, vol. 13, pp. 1932-1939, 2019.

[6] S. L. Zhang, M. Xu, C. Zhang, Y.-C. Wang, H. Zou, X. He, *et al.*, "Rationally designed sea snake structure based triboelectric nanogenerators for effectively and efficiently harvesting ocean wave energy with minimized water screening effect," *Nano Energy*, vol. 48, pp. 421-429, 2018.

[7] F. Xi, Y. Pang, G. Liu, S. Wang, W. Li, C. Zhang, *et al.*, "Self-powered intelligent buoy system by water wave energy for sustainable and autonomous wireless sensing and data transmission," *Nano Energy*, vol. 61, pp. 1-9, 2019.

[8] X. Yang, L. Xu, P. Lin, W. Zhong, Y. Bai, J. Luo, *et al.*, "Macroscopic self-assembly network of encapsulated high-performance triboelectric nanogenerators for water wave energy harvesting," *Nano Energy*, vol. 60, pp. 404-412, 2019.

[9] Y. Wu, Q. Zeng, Q. Tang, W. Liu, G. Liu, Y. Zhang, *et al.*, "A teeterboard-like hybrid nanogenerator for efficient harvesting of low-frequency ocean wave energy," *Nano Energy*, vol. 67, p. 104205, 2020.

[10] L. Feng, G. Liu, H. Guo, Q. Tang, X. Pu, J. Chen, *et al.*, "Hybridized nanogenerator based on honeycomb-like three electrodes for efficient ocean wave energy harvesting," *Nano Energy*, vol. 47, pp. 217-223, 2018.

[11] R. B. Mayon, "Investigation of wave impacts on porous structures for coastal defences," University of Southampton, 2017.

[12] U. T. Jurado, S. H. Pu, and N. M. White, "A contact-separation mode triboelectric nanogenerator for ocean wave impact energy harvesting," in *2017 IEEE SENSORS*, 2017, pp. 1-3.

[13] U. T. Jurado, S. H. Pu, and N. M. White, "Dielectric-metal triboelectric nanogenerators for ocean wave impact self-powered applications," *IEEE Sensors Journal*, 2019.

[14] U. T. Jurado, S. H. Pu, and N. M. White, "Water-Dielectric Single Electrode Mode Triboelectric Nanogenerators for Ocean Wave Impact Energy Harvesting," in *Multidisciplinary Digital Publishing Institute Proceedings*, 2018, p. 714.

[15] U. Khan and S.-W. Kim, "Triboelectric nanogenerators for blue energy harvesting," *ACS nano*, vol. 10, pp. 6429-6432, 2016.

[16] C. Chang, V. H. Tran, J. Wang, Y.-K. Fuh, and L. Lin, "Direct-write piezoelectric polymeric

nanogenerator with high energy conversion efficiency," *Nano letters,* vol. 10, pp. 726-731, 2010.
[17] P. Ueberschlag, "PVDF piezoelectric polymer," *Sensor review,* vol. 21, pp. 118-126, 2001.
[18] J. Lowell and A. Rose-Innes, "Contact electrification," *Advances in Physics,* vol. 29, pp. 947-1023, 1980.
[19] A. Diaz and R. Felix-Navarro, "A semi-quantitative tribo-electric series for polymeric materials: the influence of chemical structure and properties," *Journal of Electrostatics,* vol. 62, pp. 277-290, 2004.
[20] Y. Yu and X. Wang, "Chemical modification of polymer surfaces for advanced triboelectric nanogenerator development," *Extreme Mechanics Letters,* vol. 9, pp. 514-530, 2016.
[21] P. Bai, G. Zhu, Y. S. Zhou, S. Wang, J. Ma, G. Zhang, *et al.*, "Dipole-moment-induced effect on contact electrification for triboelectric nanogenerators," *Nano Research,* vol. 7, pp. 990-997, 2014.
[22] Q. Nguyen, B. H. Kim, and J. W. Kwon, "based ZnO nanogenerator using contact electrification and piezoelectric effects," *Journal of Microelectromechanical Systems,* vol. 24, pp. 519-521, 2015.
[23] M. Han, X. Zhang, W. Liu, X. Sun, X. Peng, and H. Zhang, "Low-frequency wide-band hybrid energy harvester based on piezoelectric and triboelectric mechanism," *Science China Technological Sciences,* vol. 56, pp. 1835-1841, 2013.
[24] Z. L. Wang, T. Jiang, and L. Xu, "Toward the blue energy dream by triboelectric nanogenerator networks," *Nano Energy,* vol. 39, pp. 9-23, 2017.
[25] L. Xu, T. Jiang, P. Lin, J. J. Shao, C. He, W. Zhong, *et al.*, "Coupled triboelectric nanogenerator networks for efficient water wave energy harvesting," *ACS nano,* vol. 12, pp. 1849-1858, 2018.
[26] J. Chen, J. Yang, Z. Li, X. Fan, Y. Zi, Q. Jing, *et al.*, "Networks of triboelectric nanogenerators for harvesting water wave energy: a potential approach toward blue energy," *ACS nano,* vol. 9, pp. 3324-3331, 2015.
[27] S. Park, Y. Kim, H. Jung, J.-Y. Park, N. Lee, and Y. Seo, "Energy harvesting efficiency of piezoelectric polymer film with graphene and metal electrodes," *Scientific reports,* vol. 7, p. 17290, 2017.
[28] Z. L. Wang, L. Lin, J. Chen, S. Niu, and Y. Zi, "Theoretical Modeling of Triboelectric Nanogenerators," in *Triboelectric Nanogenerators*, ed: Springer, 2016, pp. 155-183.
[29] S. Niu, S. Wang, L. Lin, Y. Liu, Y. S. Zhou, Y. Hu, *et al.*, "Theoretical study of contact-mode triboelectric nanogenerators as an effective power source," *Energy & Environmental Science,* vol. 6, pp. 3576-3583, 2013.
[30] F. Lu, H. Lee, and S. Lim, "Modeling and analysis of micro piezoelectric power generators for micro-electromechanical-systems applications," *Smart Materials and Structures,* vol. 13, p. 57, 2003.
[31] S. Wang, Y. Xie, S. Niu, L. Lin, C. Liu, Y. S. Zhou, *et al.*, "Maximum Surface Charge Density for Triboelectric Nanogenerators Achieved by Ionized□Air Injection: Methodology and Theoretical Understanding," *Advanced Materials,* vol. 26, pp. 6720-6728, 2014.
[32] A. Khaligh and O. C. Onar, *Energy harvesting: solar, wind, and ocean energy conversion systems*: CRC press, 2009.
[33] W. Tang, T. Jiang, F. R. Fan, A. F. Yu, C. Zhang, X. Cao, *et al.*, "Liquid□metal electrode for high□performance triboelectric nanogenerator at an instantaneous energy conversion efficiency of 70.6%," *Advanced Functional Materials,* vol. 25, pp. 3718-3725, 2015.
[34] Oceanweather.com, ""Current Marine Data | Oceanweather Inc"," *http://www.oceanweather.com/data/index.html,* Accessed: 30- Oct- 2018 2018 2018.
[35] E. Arano, "Ocean Water Wave Photo " *https://www.pexels.com/photo/ocean-water-wave-photo-1295138/,* 2016.
[36] D. Steingart, "Power sources for wireless sensor networks," in *Energy harvesting technologies*, ed: Springer, 2009, pp. 267-286.
[37] Z. L. Wang and W. Wu, "Nanotechnology□enabled energy harvesting for self□powered micro□/nanosystems," *Angewandte Chemie International Edition,* vol. 51, pp. 11700-11721, 2012.
[38] M. M. Damien Toner, "The Potential for Renewable Energy Usage in Aquaculture," *http://www.aquacultureinitiative.eu,* 2002.

Ulises Tronco Jurado received the M.Sc. degree in materials science from University of Guadalajara, Mexico, in 2015. He was a MEMS lab researcher at University of Texas at San Antonio, U.S., in 2014, working on modeling, synthesis, fabrication and characterization of quantum dots applied to c-silicon solar cells.

He is currently pursuing the PhD. Degree in Engineering and the Environment with the Mechatronics Research Group, and the Smart Electronic Materials and Systems Research Group, School of Electronics and Computer Science, University of Southampton, U.K. His current research interest include triboelectric nanogenerators for ocean wave monitoring applications that required self-powering.

Suan Hui Pu received Ph.D. degree in electrical and electronic engineering from Imperial College London, U.K. in 2010. He is currently an Associate Professor at University of Southampton at Johor, Malaysia.
He is a visiting academic in the Schools of Engineering, and Electronics and Computer Science, at the University of Southampton, U.K. His current research interests include NEMS/MEMS sensors and actuators, graphene/graphite sensors and printed electronics.
He has served as a reviewer for IEEE Journal of Microelectromechanical Systems, IEEE Electron Device Letters, IEEE Transactions on Components, Packaging and Manufacturing Technology, IOP Nanotechnology, IOP Journal of Micromechanics and Microengineering, amongst others.

Neil M. White obtained a PhD from the University of Southampton in 1988. Neil was promoted to Senior Lecturer in 1999. His research interests include thick-film sensors, intelligent instrumentation, MEMS, self-powered microsensors and sensor networks. He is a Chartered Engineer, Senior Member of the IEEE, and a Chartered Physicist. He is a member of the Peer Review College for the EPSRC and is on the Editorial Board of the international journals Sensor Review and Journal of Materials Science: Materials in Electronics. Professor White is also a Series Editor for the Integrated Microsystems series for Artech House.

- Improvement in the output performance of devices for ocean wave impact energy
- Simultaneously coupling triboelectric-piezoelectric effects
- Grid of hybrid devices approach for high-performance energy harvesting
- Water-hybrid nanogenerator-structure for large scale electricity generation
- Energy conversion efficiency of 30.22 %, harvesting the water wave impact energy